Free Radical Research, June 2007; 41(6): 720–729

informa
healthcare

Inhibitory effects of glycitein on hydrogen peroxide induced cell damage by scavenging reactive oxygen species and inhibiting c-Jun N-terminal kinase

KYOUNG AH KANG[1], RUI ZHANG[1], MEI JING PIAO[1], KYOUNG HWA LEE[1], BUM JOON KIM[2], SO YOUNG KIM[3], HEE SUN KIM[3], DONG HYUN KIM[4], HO JIN YOU[5], & JIN WON HYUN[1]

[1]*Department of Biochemistry, College of Medicine and Applied Radiological Science Research Institute, Cheju National University, Jeju-si 690-756, South Korea,* [2]*Department of Microbiology, Seoul National University College of Medicine, Cancer Research Institute, Seoul 110-799, South Korea,* [3]*Department of Neuroscience, College of Medicine, Ewha Womans University, Seoul 110-783, South Korea,* [4]*Department of Microbial Chemistry, College of Pharmacy, Kyung Hee University, Seoul 130-701, South Korea, and* [5]*Department of Pharmacology, College of Medicine, Chosun University, Gwangju 501-759, South Korea*

Accepted by Professor J. Yodoi

(Received 6 September 2006; in revised form 15 January 2007)

Abstract

The present study investigated the cytoprotective properties of glycitein, a metabolite formed by the transformation of glycitin by intestinal microflora, against oxidative stress. Glycitein was found to scavenge intracellular reactive oxygen species (ROS), and 1,1-diphenyl-2-picrylhydrazyl (DPPH) radical, and thereby preventing lipid peroxidation and DNA damage. Glycitein inhibited apoptosis of Chinese hamster lung fibroblast (V79-4) cells exposed to hydrogen peroxide (H_2O_2) via radical scavenging activity. Glycitein abrogated the activation of c-Jun N-terminal kinase (JNK) induced by H_2O_2 treatment and inhibited DNA binding activity of activator protein-1 (AP-1), a downstream transcription factor of JNK. Taken together, these findings suggest that glycitein protected H_2O_2 induced cell death in V79-4 cells by inhibiting ROS generation and JNK activation.

Keywords: *Cytoprotective properties, glycitein, reactive oxygen species, oxidative stress*

Introduction

Isoflavones are biologically active compounds, which occur naturally in a variety of plants. Recently, Park et al. [1] have isolated a series of isoflavonoids; glycitin, tectoridin, 6-O-xylosyltectoridin, and 6-O-xylosylglycitin from the flowers of *Pueraria thunbergiana* (Leguminosae), which have been used in Chinese medicine. As most of the traditional medicines are administered orally, their components inevitably contact the microflora of the gastrointestinal tract. Finally, most of these components are transformed by intestinal bacteria before being absorbed from gastrointestinal tract [2–9]. In this study, glycitin, a biologically active component isolated from the flowers of *P. thunbergiana*, was transformed into glycitein by human intestinal bacteria. Experimental evidences suggest that glycitein possesses many properties including estrogenic [10], antioxidant [11], hypocholesterolemic [12,13], the inhibition of

Correspondence: J. W. Hyun, Department of Biochemistry, College of Medicine and Applied Radiological Science Research Institute, Cheju National University, Jeju-si 690-756, South Korea. Tel: 82 64 754 3838. Fax: 82 64 726 4152. E-mail: jinwonh@cheju.ac.kr

ISSN 1071-5762 print/ISSN 1029-2470 online © 2007 Informa UK Ltd.
DOI: 10.1080/10715760701241618

cancer cell proliferation or invasion [14,15], inhibition of growth and DNA synthesis of aortic smooth muscle cells [16], protection against beta amyloid induced toxicity and oxidative stress [17], inhibition of prostaglandin E_2 or nitric oxide production [18,19], and the differentiation of osteoblast [20].

Reactive oxygen species (ROS) are known to cause oxidative modification of DNA, proteins, lipids and small intracellular molecules. ROS are associated with tissue damage and are the causative factors for inflammation, aging, cancer, arteriosclerosis, hypertension and diabetes [21–27]. These pathological alterations by ROS may be attributed to changes in the intracellular signaling mechanisms, for example, ROS induced c-Jun N-terminal kinase (JNK) activation has been reported in many cells [28–30]. JNK is activated by various inflammatory cytokines and environmental stresses that result in cellular hypertrophy or apoptosis [31]. The precise roles of JNK signaling pathways in the regulation of cellular phenotypic modulation, however, are still unclear and may be cell type specific [32]. Recently, it was reported that glycitein had a protective antioxidant effect against beta amyloid induced toxicity and oxidative stress in transgenic *Caenorhabditis elegans* [17]. However, the precise mechanisms of the glycitein effect against oxidative stress have not been elucidated. In the present study, we report the result of our investigation of the protective effect of glycitein on cell damage induced by hydrogen peroxide in Chinese hamster lung fibroblast (V79-4) cells and the likely protective mechanism.

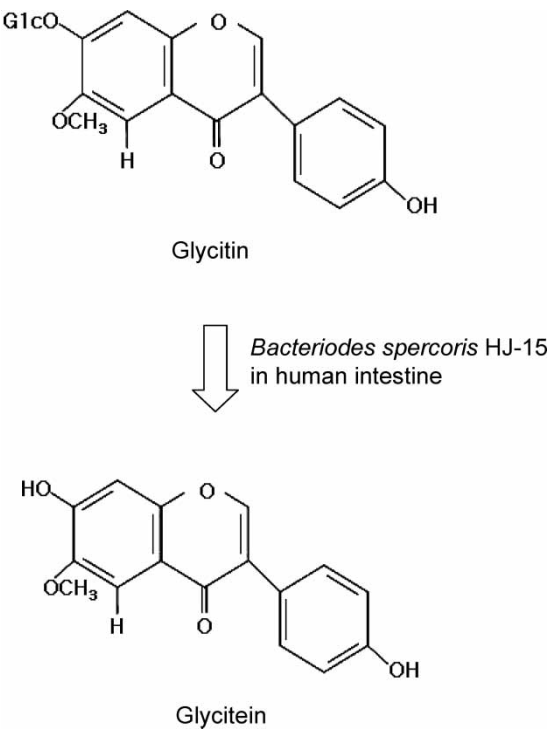

Figure 1. Metabolic formation of glycitein. Glycitein is formed by the transformation of glycitin by *B. spercoris* HJ-15, a human intestinal bacterium.

Materials and methods

Preparation of glycitin and glycitein

Glycitin was isolated from dried flowers of *P. thunbergiana* according to the method of Lee et al. [33]. To obtain the metabolites of glycitin by human intestinal microflora, a reaction mixture was prepared containing 1 g of glycitin and *Bacteriodes spercoris* HJ-15, a human intestinal bacterium, in a final volume of 500 ml of anaerobic dilution medium in an anaerobic glove box (Coy Laboratory Products Inc). The reaction mixture was incubated at 37°C for 24 h and extracted three times with ethyl acetate. The ethyl acetate-soluble portion of the reaction mixture was dried on a rotary evaporator under reduced pressure, and subjected to silica gel column chromatography (2.5 × 15 cm) with $CHCl_3$/MeOH (10:1–10:2) as mobile phase. Glycitin (0.12 g) and glycitein (0.15 g) were obtained from these fractions (Figure 1) and were identified according to the previously reported method [1]. The purity of glycitein (>95%) was analyzed by HPLC system μ-Bondapak C18 (3.9 × 300 mm); elution solvent, 50% methanol; elution rate, 1.0 ml/min; detection wavelength, 254 nm.

The characteristics of glycitein are: yellow amorphous powder; mp 170–180°C; UV λ_{max}(MeOH) (log ε) 211.4 nm (4.29), 231.6 nm (4.18), 260.2 nm (4.30), 319.0 nm (3.94). IR $(KBr)_{max}$ 3472, 1635, 1520, 1419, 1373, 1232, 1207, 1178 cm^{-1}.

Reagents

The 1,1-diphenyl-2-picrylhydrazyl (DPPH) radical, 2′,7′-dichlorodihydrofluorescein diacetate (DCF-DA), and Hoechst 33342 were purchased from the Sigma Chemical Company, and thiobarbituric acid (TBA) from BDH Laboratories. Primary anti-JNK, anti-phospho JNK, anti-PARP, and anti-caspase 3 antibodies were purchased from Cell Signaling Technology. Primary anti-actin and anti-bcl-2 antibodie were purchased from Santa Cruz Biotechnology and anti-phosphor H2A.X antibody was purchased from Upstate Biotechnology. The plasmid containing the AP-1 binding site-luciferase construct was a generous gift of Dr. Young Joon Surh (Seoul National University, Seoul, Korea).

Cell culture

The Chinese hamster lung fibroblast cells (V79-4) were obtained from the American Type Culture Collection. The V79-4 cells were maintained at 37°C

in an incubator, with a humidified atmosphere of 5% CO_2, and cultured in Dulbecco's modified Eagle's medium containing 10% heat-inactivated fetal calf serum, streptomycin (100 μg/ml) and penicillin (100 units/ml).

Intracellular reactive oxygen species (ROS) measurement

The DCF-DA method was used to detect the levels of intracellular ROS [34]. The V79-4 cells were seeded in a 96 well plate at 2×10^4 cells/well. At 16 h after plating, the cells were treated with glycitin or glycitein at 0.1, 1 and 10 μg/ml, and 30 min later, 1 mM H_2O_2 was added to the plate. The cells were incubated for an additional 30 min at 37°C. After addition of 25 μM of DCF-DA solution for 10 min, the fluorescence of 2′,7′-dichlorofluorescein was detected at 485 nm excitation and at 535 nm emission using a Perkin Elmer LS-5B spectrofluorometer. The intracellular ROS scavenging activity (%) was calculated as [(optical density of H_2O_2 treatment) − (optical density of glycitein + H_2O_2 treatment)]/(optical density of H_2O_2 treatment) × 100.

For image analysis for generation of intracellular ROS, the cells were seeded on cover-slip loaded six well plate at 2×10^5 cells/well. At 16 h after plating, the cells were treated with glycitein and 30 min later, 1 mM H_2O_2 was added to the plate. After changing the media, 100 μM of DCF-DA was added to each well and was incubated for an additional 30 min at 37°C. After washing with PBS, the stained cells were mounted onto microscope slide in mounting medium (DAKO). Images were collected using the Laser Scanning Microscope 5 PASCAL program (Carl Zeiss) on a confocal microscope.

DPPH radical scavenging activity

Glycitin or glycitein at 0.1, 1 and 10 μg/ml were added to a 1×10^{-4} M solution of DPPH in methanol, and the reaction mixture shaken vigorously. After 30 min, the amount of remaining DPPH was determined at 520 nm using a spectrophotometer [35]. The DPPH radical scavenging activity (%) was calculated as [(optical density of DPPH radical treatment) − (optical density of glycitein + DPPH radical treatment)]/(optical density of DPPH radical treatment) × 100.

Lipid peroxidation assay

Lipid peroxidation was assayed by the TBA reaction [36]. The cells were then washed with cold phosphate buffered saline (PBS), scraped and homogenized in ice-cold 1.15% KCl. About 100 μl of the cell lysates was mixed with 0.2 ml of 8.1% sodium dodecylsulfate, 1.5 ml of 20% acetic acid (adjusted to pH 3.5) and 1.5 ml of 0.8% TBA. The mixture was made up to a final volume of 4 ml with distilled water and heated to 95°C for 2 h. After cooling to room temperature, 5 ml of *n*-butanol and pyridine mixture (15:1, v/v) was added to each sample, and the mixture was shaken. After centrifugation at 1000*g* for 10 min, the supernatant fraction was isolated, and the absorbance measured spectrophotometrically at 532 nm. Amount of thiobarbituric acid reactive substance (TBARS) was determined using standard curve with 1,1,3,3,-tetrahydroxypropane.

Comet assay

A Comet assay was performed to assess oxidative DNA damage [37,38]. The cell pellet (1.5×10^5 cells) was mixed with 100 μl of 0.5% low melting agarose (LMA) at 39°C and spread on a fully frosted microscopic slide that was pre-coated with 200 μl of 1% normal melting agarose (NMA). After solidification of the agarose, the slide was covered with another 75 μl of 0.5% LMA and then immersed in lysis solution (2.5 M NaCl, 100 mM Na–EDTA, 10 mM Tris, 1% Trion X-100, and 10% DMSO, pH 10) for 1 h at 4°C. The slides were then placed in a gel-electrophoresis apparatus containing 300 mM NaOH and 10 mM Na–EDTA (pH 13) for 40 min to allow DNA unwinding and the expression of the alkali labile damage. An electrical field was applied (300 mA, 25 V) for 20 min at 4°C to draw negatively charged DNA toward an anode. After electrophoresis, the slides were washed three times for 5 min at 4°C in a neutralizing buffer (0.4 M Tris, pH 7.5) and then stained with 75 μl of ethidium bromide (20 μg/ml). The slides were observed using a fluorescence microscope and image analysis (Komet). The percentage of total fluorescence in the tail and the tail length of the 50 cells per slide were recorded.

Western blot

The cells were harvested, and washed twice with PBS. The harvested cells were then lysed on ice for 30 min in 100 μl of a lysis buffer (120 mM NaCl, 40 mM Tris (pH 8), 0.1% NP 40) and centrifuged at 13,000*g* for 15 min. Supernatants were collected from the lysates and protein concentrations were determined. Aliquots of the lysates (40 μg of protein) were boiled for 5 min and electrophoresed in 10% sodium dodecysulfate-polyacrylamide gel. Blots in the gels were transferred onto nitrocellulose membranes (Bio-Rad), which were then incubated with primary antibodies. The membranes were further incubated with secondary immunoglobulin-G–horseradish peroxidase conjugates (Pierce). Protein bands were detected using an enhanced chemiluminescence Western blotting detection kit (Amersham), and then exposed to X-ray film.

Immunocytochemistry

Cells plated on coverslips were fixed with 4% paraformaldehyde for 30 min and permeabilized with 0.1% Triton X-100 in PBS for 2.5 min. Cells were treated with blocking medium (3% bovine serum albumin in PBS) for 1 h and incubated with anti-phospho histone H2A.X antibody diluted in blocking medium for 2 h. Immunoreactive primary phospho histone H2A.X antibody was detected by a 1:500 dilution of FITC-conjugated secondary antibody (Jackson ImmunoResearch Laboratories) for 1 h. After washing with PBS, the stained cells were mounted onto microscope slides in mounting medium with DAPI (Vector). Images were collected using the Laser Scanning Microscope 5 PASCAL program (Carl Zeiss) on a confocal microscope.

Cell viability

The effect of glycitein on the viability of the V79-4 cells was determined using the [3-(4,5-dimethylthiazol-2-yl)-2,5-diphenyltetrazolium] bromide (MTT) assay [39]. About, 50 μl of the MTT stock solution (2 mg/ml) was then added into each well to attain a total reaction volume of 200 μl. After incubating for 4 h, the plate was centrifuged at 800*g* for 5 min and the supernatants were aspirated. The formazan crystals in each well were dissolved in 150 μl of dimethylsulfoxide and read at A_{540} on a scanning multi-well spectrophotometer.

Nuclear staining with Hoechst 33342

About 1.5 μl of Hoechst 33342 (stock 10 mg/ml), a DNA specific fluorescent dye, was added to each well (1.5 ml) and incubated for 10 min at 37°C. The stained cells were then observed under a fluorescent microscope, which was equipped with a CoolSNAP-Pro color digital camera, in order to examine the degree of nuclear condensation.

Flow cytometry analysis

Flow cytometry was performed to determine the content of apoptotic sub G_1 hypo-diploid cells [40]. The cells were harvested, and fixed in 1 ml of 70% ethanol for 30 min at 4°C. The cells were washed twice with PBS, and then incubated for 30 min in dark at 37°C in 1 ml of PBS containing 100 μg propidium iodide and 100 μg RNase A. Flow cytometric analysis was performed using a FACSCalibur flow cytometer (Becton Dickinson). The proportion of sub G_1 hypo-diploid cells was assessed by the histograms generated using the computer program, Cell Quest and Mod-Fit.

DNA fragmentation

Cellular DNA-fragmentation was assessed by analysis of the cytoplasmic histone-associated DNA fragmentation using a kit from Roche Diagnostics according to the manufacturer's instructions.

Preparation of nuclear extract and electrophoretic mobility shift assay

The cells were harvested, and were then lysed on ice with 1 ml of lysis buffer (10 mM Tris–HCl, pH 7.9, 10 mM NaCl, 3 mM $MgCl_2$, and 1% NP-40) for 4 min. After 10 min of centrifugation at 3000*g*, the pellets were resuspended in 50 μl of extraction buffer (20 mM HEPES, pH 7.9, 20% glycerol, 1.5 mM $MgCl_2$, 0.2 mM EDTA, 1 mM DTT, and 1 mM PMSF), incubated on ice for 30 min, and centrifuged at 13,000*g* for 5 min. The supernatant (nuclear protein) stored at −70°C after determination of protein concentration. Oligonucleotides containing the transcription factor AP-1 consensus sequence (5′-CGC TTG ATG ACT CAG CCG GAA-3′) were annealed, labeled with [γ-^{32}P] ATP using T4 polynucleotide kinase, and used as probes. The probes (50,000 cpm) were incubated with 6 μg of the nuclear extracts at 4°C for 30 min in a final volume of 20 μl containing 12.5% glycerol, 12.5 mM HEPES (pH 7.9), 4 mM Tris–HCl (pH 7.9), 60 mM KCl, 1 mM EDTA, and 1 mM DTT with 1 μg of poly (dI–dC). Binding products were resolved on 5% polyacrylamide gel and the bands were visualized by autoradiography.

Transient transfection and AP-1 luciferase assay

The cells were transiently transfected with the plasmid harboring the AP-1 promoter using DOTAP as the transfection reagent according to the instructions given by the manufacturer (Roche Diagnostics). After overnight transfection, the cells were treated with 10 μg/ml of glycitein. After a further incubation for 1 h, 1 mM H_2O_2 was added to the culture. After 6 h, the cells were then washed twice with PBS and lysed with reporter lysis buffer (Promega). After vortex-mixing and centrifugation at 12,000*g* for 1 min at 4°C, the supernatant was stored −70°C for the luciferase assay. After 20 μl of the cell extract was mixed with 100 μl of the luciferase assay reagent at room temperature, the mixture was placed in a illuminometer to measure the light produced.

Statistical analysis

All the measurements were made in triplicate and all values were represented as means ± standard error. The results were subjected to an analysis of the variance (ANOVA) using the Tukey test to analyze the

differences. $p < 0.05$ were considered to be significant.

Results

Radical scavenging activity of glycitin and glycitein

The scavenging effects of glycitin and glycitein on the intracellular ROS and DPPH free radical were compared. The intracellular ROS scavenging activity of glycitin was 27% at 0.1 μg/ml, 34% at 1 μg/ml, and 48% at 10 μg/ml. In the case of glycitein, it was 47% at 0.1 μg/ml, 55% at 1 μg/ml, and 67% at 10 μg/ml (Figure 2A). As shown in Figure 2B, the fluorescence intensity of DCF-DA staining was enhanced in H_2O_2 treated V79-4 cells. Glycitein reduced the red fluorescence intensity upon H_2O_2 treatment, thus reflecting a reduction in ROS generation. The DPPH

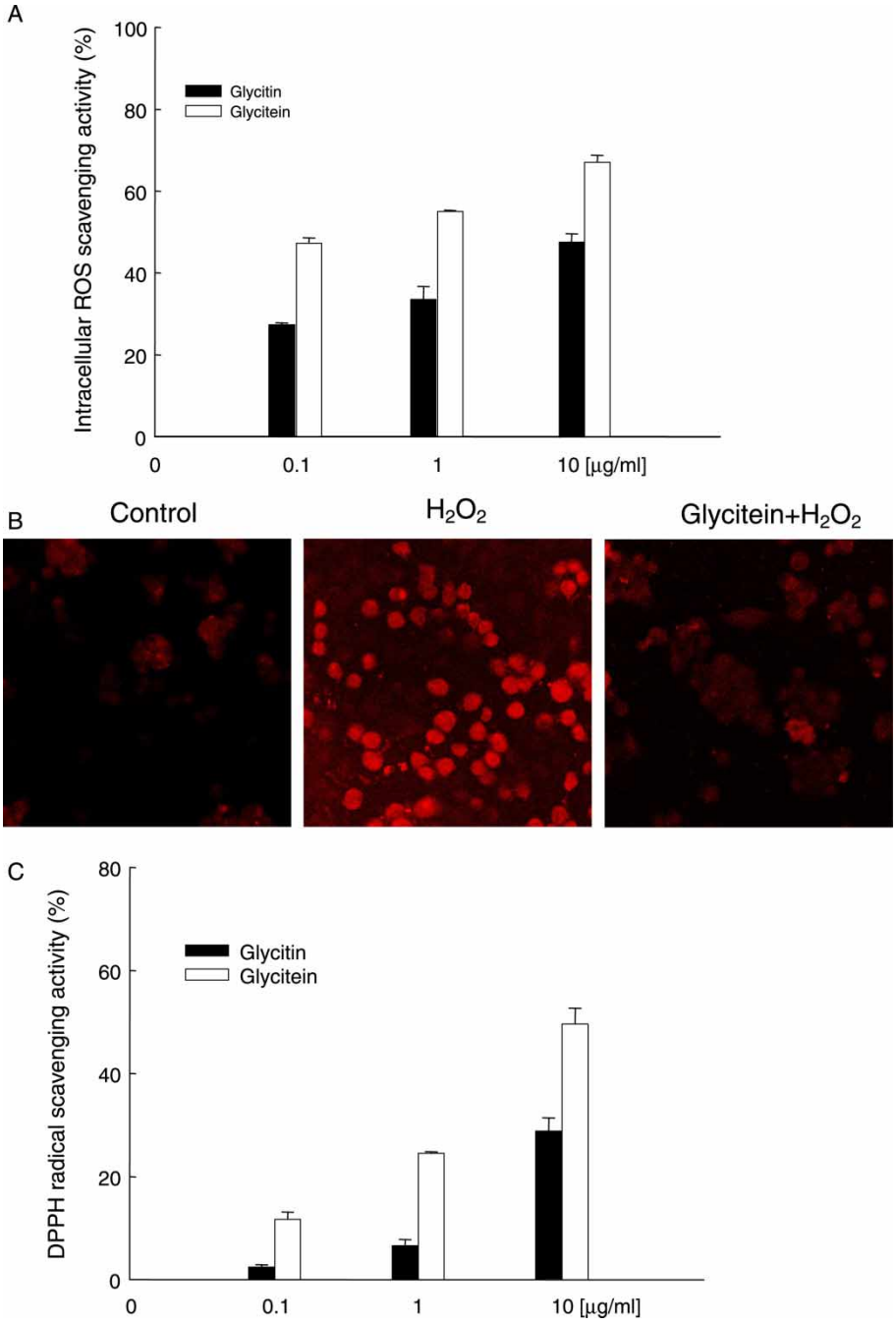

Figure 2. Effect of glycitin and glycitein on scavenging intracellular ROS and DPPH radicals. (A) The intracellular ROS generated was detected by the DCF-DA method. (B) Representative confocal images illustrate the increase in red fluorescence intensity of DCF produced by ROS in H_2O_2 treated cells as compared to control and the lowered fluorescence intensity in H_2O_2 treated cells with glycitein (original magnification × 400). (C) The amount of DPPH radicals was determined spectrophotometrically at 520 nm. The measurements were made in triplicate and values are expressed as means ± standard error.

radical scavenging activity of glycitin showed 2% at 0.1 μg/ml, 7% at 1 μg/ml, and 29% at 10 μg/ml, and for glycitein, it was 11% at 0.1 μg/ml, 25% at 1 μg/ml, 50% at 10 μg/ml (Figure 2C). The radical scavenging effect of glycitein in both the experiments, however, was more effective when compared to glycitin. Based on these results, we selected glycitein as the active compound for further studies on radical scavenging effect.

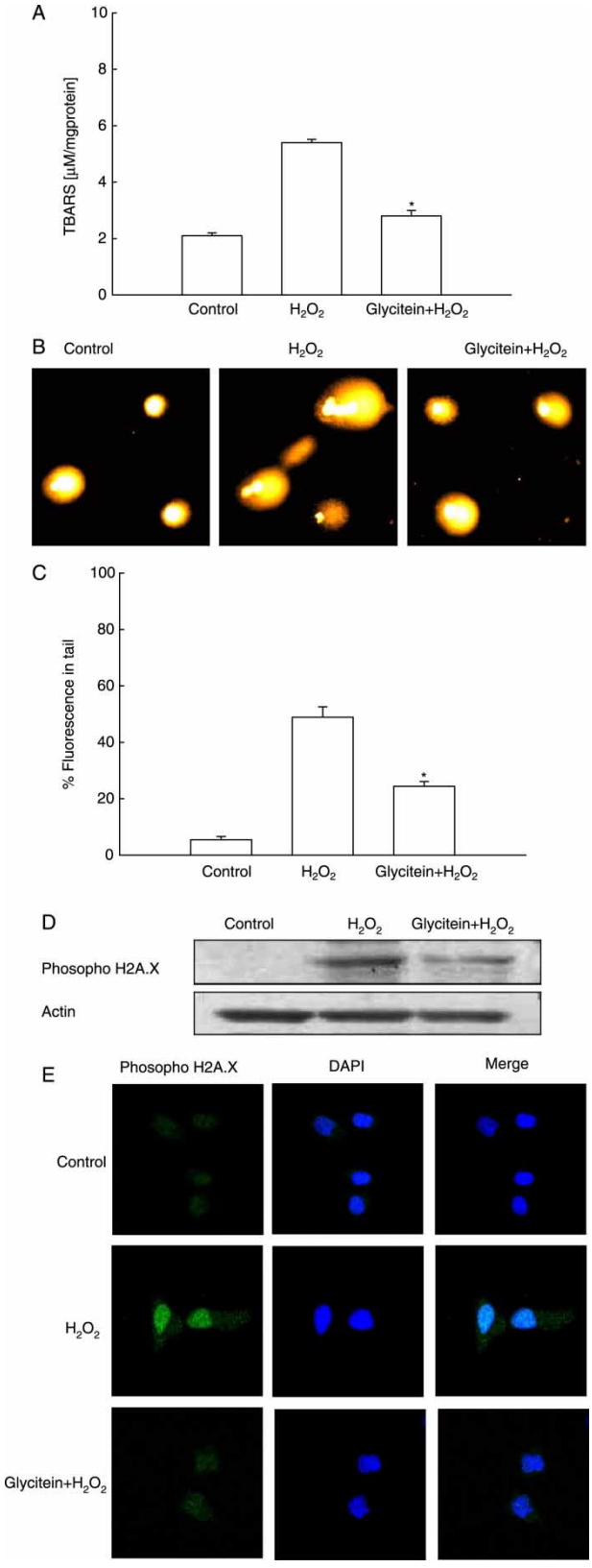

Figure 3. Effect of glycitein on inhibition of lipid peroxidation and DNA damage. (A) Lipid peroxidation was assayed by measuring the amount of TBARS formation. The measurements were made in triplicate and the values expressed as means ± standard error. *significantly different from H_2O_2 treated cells ($p < 0.05$). (B) Representative images and (C) percentage of cellular DNA damage were detected by an alkaline comet assay. *Significantly different from H_2O_2 treated cells ($p < 0.05$). (D) Cell lysates were electrophoresed and phospho H2A.X protein was detected by specific antibody. (E) Confocal image shows that FITC-conjugated secondary antibody staining indicates the location of phospho H2A.X (green) by anti-phospho H2A.X antibody, DAPI staining indicates the location of the nucleus (blue), and the merged image indicates the location of the phospho H2A.X protein in nucleus.

Effect of glycitein on lipid peroxidation and cellular DNA damage induced by H_2O_2

The abilities of glycitein to inhibit membrane lipid peroxidation and cellular DNA damage in H_2O_2 treated cells were investigated. H_2O_2 induced damage to cell membrane, one of the most important lesions, responsible for the loss of cell viability. The peroxidation of membrane lipids is the major lesion in the membranes. As shown in Figure 3A, V79-4 cells exposed to H_2O_2 showed an increase in the lipid peroxidation, which was monitored by the generation of TBARS. However, glycitein prevented the H_2O_2-induced peroxidation of lipids. Damage to cellular DNA induced by H_2O_2 exposure was detected by using an alkaline comet assay and assessing phospho histone-H2A.X expression. The exposure of cells to H_2O_2 increased the comet parameters of tail length and percentage of DNA in the tails of the cells. When the cells were exposed to H_2O_2, the percent of DNA in the tail was increased 49% as shown in Figure 3B and C. Treatment with glycitein resulted in a decrease to 24%, which indicated a protective effect of glycitein on H_2O_2-induced DNA damage. In addition, the phosphorylation of nuclear histone H2A.X, a sensitive marker for breaks of double stranded DNA [41], increased in the H_2O_2 treated cells as shown by Western blot and immuno-fluorescence results (Figure 3D and E). However, glycitein in H_2O_2 treated cells decreased the expression of phospho H2A.X, thereby indicating a protective effect of glycitein on H_2O_2-induced DNA damage.

Effect of glycitein on cell death induced by H_2O_2

The protective effect of glycitein on cell survival in H_2O_2 treated cells was measured. Cells were treated with glycitein at 10 μg/ml for 1 h, prior to the addition of H_2O_2. Cell viability was determined 24 h later by

the MTT assay. As shown in Figure 4A, treatment with glycitein increased the cell survival by 79% as compared to 57% of H_2O_2 treatment. To evaluate a cytoprotective effect of glycitein on apoptosis induced by H_2O_2, the nuclei of V79-4 cells were stained with Hoechst 33342 and assessed by microscopy. The microscopic pictures in Figure 4B showed that the control cells had intact nuclei, while H_2O_2 treated cells showed significant nuclear fragmentation, which is characteristic of apoptosis. When the cells were treated with glycitein for 1 h prior to H_2O_2 treatment, however, a decrease in nuclear fragmentation was observed. In addition to the morphological evaluation, the protective effect of glycitein against apoptosis was also confirmed by flow cytometric analysis and by ELISA based quantification of cytoplasmic histone-associated DNA fragmentation. As shown in Figure 4C, an analysis of the DNA content in the H_2O_2 treated cells revealed an increase by 55% of apoptotic sub-G_1 DNA content. Treatment with 10 μg/ml of glycitein decreased the apoptotic sub-G_1 DNA content to 41%. Treatment of cells with H_2O_2 increased the levels of cytoplasmic histone-associated DNA fragmentations compared to control group, however, treatment with 10 μg/ml of glycitein decreased the level of DNA fragmentation (Figure 4D). To understand how glycitein protects H_2O_2 induced apoptosis, we examined changes of Bcl-2 and caspase 3 by Western blot. As shown in Figure 4E, the Bcl-2, an anti-apoptotic protein, recovered in treatment with glycitein and H_2O_2 treatment compared to H_2O_2 treated cells. It was also observed the decreased activation of caspase 3 (17 kDa), the major effecter caspase of the apoptotic process, and PARP cleavage (89 kDa), one of substrates of activated caspase 3, in combination with glycitein and H_2O_2 treatment compared to H_2O_2 treated cells. These results suggest, therefore, that glycitein protects cell viability by inhibiting H_2O_2 induced apoptosis.

Effect of glycitein on H_2O_2 induced JNK and AP-1 activation

Activation of JNK is a crucial signaling event that mediates H_2O_2 induced apoptosis. We examined the effect of glycitein on expression of phospho JNK induced by H_2O_2. The cells were pretreated with glycitein for 1 h prior to H_2O_2 treatment and incubated for 6 h. After stimulation by H_2O_2, a phospho form of JNK protein was detected, however, glycitein pretreatment with H_2O_2 decreased the expression of phospho JNK protein (Figure 5A). It has been reported that JNK activation leads to c-Jun phosphorylation, which constitutes a transcription factor AP-1 [42]. AP-1 is a downstream target of the phospho-JNK pathway and activated AP-1 is involved in cell death, including apoptosis [43]. We subsequently

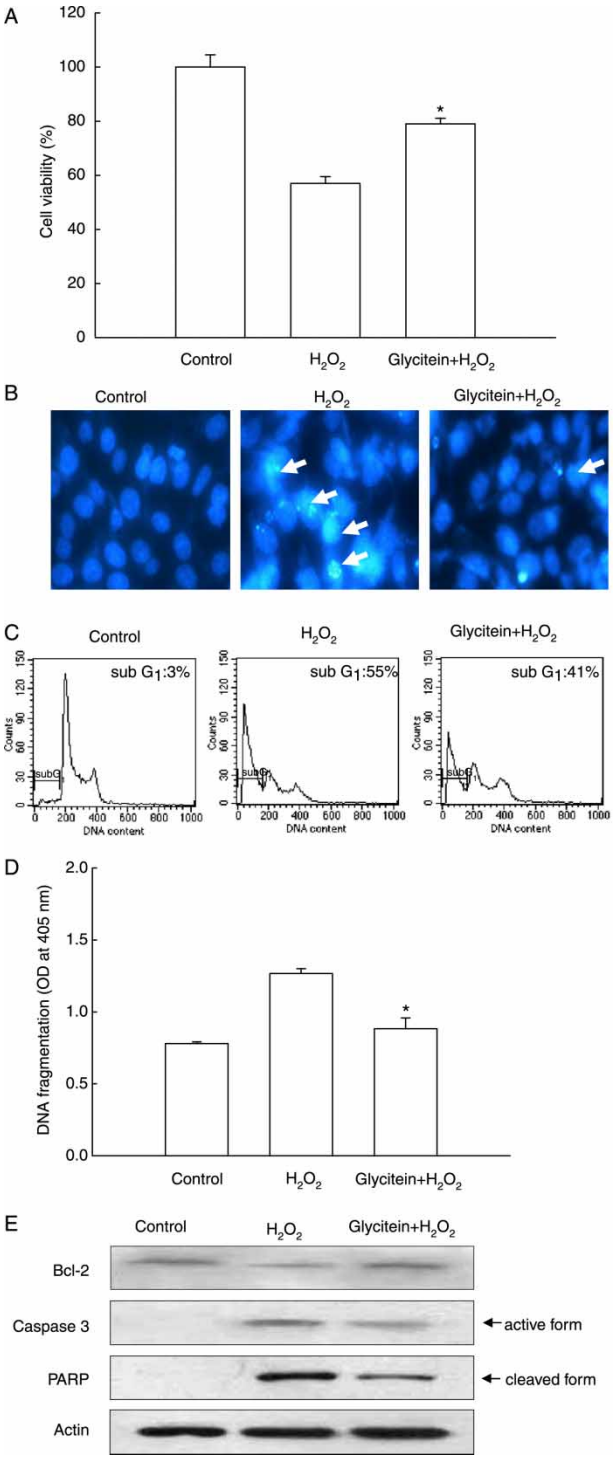

Figure 4. Protective effect of glycitein on H_2O_2 induced cell damage. (A) The viability of V79-4 cells on H_2O_2 treatment was determined by MTT assay. (B) Apoptotic body formation was observed under a fluorescent microscope after Hoechst 33342 staining Apoptotic bodies are indicated by arrows. (C) Apoptotic sub-G_1 DNA content was detected by flow cytometry after propidium iodide staining and (D) DNA fragmentation was quantified by ELISA kit. The measurements were made in triplicate and values are expressed as means ± standard error. *Significantly different from H_2O_2 treated cells ($p < 0.05$). (E) Western blot analysis was performed using anti-Bcl-2, -caspase 3 and —PARP antibodies.

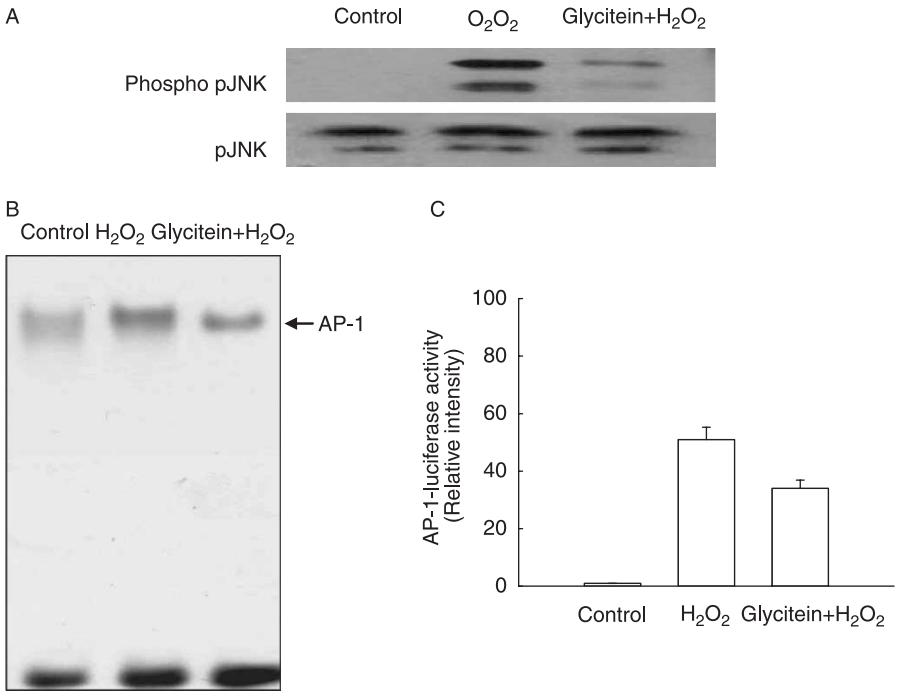

Figure 5. Effect of glycitein on H_2O_2 induced JNK and AP-1 activation. (A) Cell lysates were electrophoresed and cell lysates were immunoblotted using anti-phospho JNK and anti-JNK antibodies. (B) AP-1 specific oligonucleotide-protein complexes were detected by electrophoresis mobility shift assay. (C) Transcriptional activity of AP-1 was assessed using plasmid containing the AP-1 binding site-luciferase construct.

examined the effect of glycitein on the DNA binding activity of AP-1. As shown in Figure 5B, treatment of cells with H_2O_2 increased AP-1 activation, but glycitein inhibited AP-1 activity. The transcriptional activity of AP-1 was also assessed using a promoter construct containing the AP-1 binding DNA consensus site linked to a luciferase reporter gene. As illustrated in Figure 5C, glycitein inhibited the transcriptional activity of AP-1. These results suggest that glycitein inhibits H_2O_2 induced cell death via suppressing JNK and AP-1 activation.

Discussion

In this study, glycitein (aglycon), an isoflavone metabolite formed from the transformation of glycitin (glycoside) by intestinal microflora, demonstrated a more potent antioxidant effect than did glycitin, which suggests that the aglycon form may possess active biological activity. In general, hydrophilic compounds with sugar moieties are not easily permeable to cell membrane [44], and hence glycosides are not easily absorbed from the gastrointestinal tract. Some reports suggest that an aglycon form has a more active biological property compared to the glycon form [45–48]. Although glycitein exhibits the antioxidant effects on free radicals [4], there is lack of evidence supporting glycitein to inhibit formation of ROS on H_2O_2 induced cells. In our study, glycitein was found to decrease the intracellular ROS and DPPH radical levels. The cells exposed to H_2O_2 exhibited the distinct morphological features of apoptosis, such as nuclear fragmentation and sub G_1-hypodiploid cells. Cells that were pretreated with glycitein, however, had significantly reduced percentage of apoptotic cells, as shown by morphology and the reduction in sub G_1 DNA and DNA fragments. These findings suggest that glycitein inhibited H_2O_2 induced apoptosis through its ROS scavenging effect. To further analyze the molecular mechanism underlying inhibitory effect of apoptosis by glycitein, we investigated JNK and AP-1 signaling pathway. JNK and AP-1 activation was suggested to be critical components in the oxidative stress induced apoptosis process [42]. Activated JNK can phosphorylate c-Jun on serine 63 and 73 (p-c-Jun), which is a component of AP-1 [49]. In the present study, H_2O_2 treatment induced a phospho form of JNK, however, glycitein decreased the expression of phospho JNK protein. In addition, gel mobility shift analysis and AP-1 promoter assay revealed that increase in the DNA binding activity and transcriptional activity of AP-1 induced by H_2O_2 was inhibited by glycitein, suggesting that JNK and AP-1 pathway may be involved in the protective effect of glycitein on cell apoptosis.

In conclusion, we showed that glycitein, a metabolite of glycitin, attenuates H_2O_2 induced cell death including apoptosis through the inhibition of the ROS-mediated JNK and AP-1 signaling pathway in V79-4 cells.

Acknowledgements

This research was supported by the study of the DNA repair regulation with disease program and by the program of Basic Atomic Energy Research Institute (BAERI) which is a part of the Nuclear R&D programs grant from the Ministry of Science and Technology of Korea.

References

[1] Park HJ, Park JH, Moon JO, Lee KJ, Jung WT, Lee HK, Oh SR. Isoflavone glycosides from the flowers of *Pueraria thunbergiana*. Phytochemistry 1999;51:147–151.
[2] Akao T, Kobashi K, Aburada M. Enzymic studies on the animal and intestinal bacterial metabolism of geniposide. Biol Pharm Bull 1994;17:1573–1576.
[3] Kim DH, Yu KW, Bae EA, Park HJ, Choi JW. Metabolism of kalopanaxsaponin B and H by human intestinal bacteria and antidiabetic activity of their metabolites. Biol Pharm Bull 1998;21:360–365.
[4] Rufer CE, Kulling SE. Antioxidant activity of isoflavones and their major metabolites using different *in vitro* assays. J Agric Food Chem 2006;54:2926–2931.
[5] Chang YC, Nair MG. Metabolism of daidzein and genistein by intestinal bacteria. J Nat Prod 1995;58:1892–1896.
[6] Joannou GE, Kelly GE, Reeder AY, Waring M, Nelson C. A urinary profile study of dietary phytoestrogens. The identification and mode of metabolism of new isoflavonoids. J Steroid Biochem Mol Biol 1995;54:167–184.
[7] Heinonen SM, Hoikkala A, Wahala K, Adlercreutz H. Metabolism of the soy isoflavones daidzein, genistein and glycitein in human subjects. Identification of new metabolites having an intact isoflavonoid skeleton. J Steroid Biochem Mol Biol 2003;87:285–299.
[8] Kulling SE, Honig DM, Simat TJ, Metzler M. Oxidative *in vitro* metabolism of the soy phytoestrogens daidzein and genistein. J Agric Food Chem 2000;48:4963–4972.
[9] Kulling SE, Honig DM, Metzler M. Oxidative metabolism of the soy isoflavones daidzein and genistein in humans *in vitro* and *in vivo*. J Agric Food Chem 2001;49:3024–3033.
[10] Song TT, Hendrich S, Murphy PA. Estrogenic activity of glycitein, a soy isoflavone. J Agric Food Chem 2002;50: 2470–2474.
[11] Carroll KK. Review of clinical studies on cholesterol-lowering response to soy protein. J Am Diet Assoc 1991;91:820–827.
[12] Anthony MS, Clarkson TB, Williams JK. Effects of soy isoflavones on atherosclerosis: Potential mechanisms. Am J Clin Nutr 1998;68:1390S–1393S.
[13] Sung JH, Lee SJ, Park KH, Moon TW. Isoflavones inhibit 3-hydroxy-3-methylglutaryl coenzyme A reductase *in vitro*. Biosci Biotechnol Biochem 2004;68:428–432.
[14] Kim MH, Gutierrez AM, Goldfarb RH. Different mechanisms of soy isoflavones in cell cycle regulation and inhibition of invasion. Anticancer Res 2002;22:3811–3817.
[15] Magee PJ, McGlynn H, Rowland IR. Differential effects of isoflavones and lignans on invasiveness of MDA-MB-231 breast cancer cells *in vitro*. Cancer Lett 2004;208:35–41.
[16] Pan W, Ikeda K, Takebe M, Yamori Y. Genistein, daidzein and glycitein inhibit growth and DNA synthesis of aortic smooth muscle cells from stroke-prone spontaneously hypertensive rats. J Nutr 2001;131:1154–1158.
[17] Gutierrez-Zepeda A, Santell R, Wu Z, Brown M, Wu Y, Khan I, Link CD, Zhao B, Luo Y. Soy isoflavone glycitein protects against beta amyloid-induced toxicity and oxidative stress in transgenic *Caenorhabditis elegans*. BMC Neurosci 2005; 6:54–62.
[18] Yamaki K, Kim DH, Ryu N, Kim YP, Shin KH, Ohuchi K. Effects of naturally occurring isoflavones on prostaglandin E2 production. Planta Med 2002;68:97–100.
[19] Sheu F, Lai HH, Yen GC. Suppression effect of soy isoflavones on nitric oxide production in Raw 264.7 macrophages. J Agric Food Chem 2001;49:1767–1772.
[20] Yoshida H, Teramoto T, Ikeda K, Yamori Y. Glycitein effect on suppressing the proliferation and stimulating the differentiation of osteoblastic MC3T3-E1 cells. Biosci Biotechnol Biochem 2001;65:1211–1213.
[21] Cooke MS, Mistry N, Wood C, Herbert KE, Lunec J. Immunogenicity of DNA damaged by reactive oxygen species implications for anti-DNA antibodies in lupus. Free Radic Biol Med 1997;22:151–159.
[22] Darley-Usmar V, Halliwell B. Blood radicals: Reactive nitrogen species, reactive oxygen species, transition metal ions, and the vascular system. Pharm Res 1996;13:649–662.
[23] Farinati F, Cardin R, Degan P, Rugge M, Mario FD, Bonvicini P, Naccarato R. Oxidative DNA damage accumulation in gastric carcinogenesis. Gut 1998;42:351–356.
[24] Laurindo FR, da Luz PL, Uint L, Rocha TF, Jaeger RG, Lopes EA. Evidence for superoxide radical-dependent coronary vasospasm after angioplasty in intact dogs. Circulation 1991;83:1705–1715.
[25] Nakazono K, Watanabe N, Matsuno K, Sasaki J, Sato T, Inoue M. Does superoxide underlie the pathogenesis of hypertension. Proc Natl Acad Sci USA 1991;88:10045–10048.
[26] Palinski W, Miller E, Witztum JL. Immunization of low density lipoprotein (LDL) receptor-deficient rabbits with homologous malondialdehyde-modified LDL reduces atherogenesis. Proc Natl Acad Sci USA 1995;92:821–825.
[27] Parthasarathy S, Steinberg D, Witztum JL. The role of oxidized low-density lipoproteins in the pathogenesis of atherosclerosis. Annu Rev Med 1992;43:219–225.
[28] Fei J, Viedt C, Soto U, Elsing C, Jahn L, Kreuzer J. Endothelin-1 and smooth muscle cells: Induction of jun amino-terminal kinase through an oxygen radical-sensitive mechanism. Arterioscler Thromb Vasc Biol 2000;20:1244–1249.
[29] Lo YY, Wong JM, Cruz TF. Reactive oxygen species mediate cytokine activation of c-Jun NH2-terminal kinases. J Biol Chem 1996;271:15703–15707.
[30] Mansat-de Mas V, Bezombes C, Quillet-Mary A, Bettaieb A, D'orgeix AD, Laurent G, Jaffrezou JP. Implication of radical oxygen species in ceramide generation, c-Jun N-terminal kinase activation and apoptosis induced by daunorubicin. Mol Pharmacol 1999;56:867–874.
[31] Kyriakis JM, Avruch J. Sounding the alarm: Protein kinase cascades activated by stress and inflammation. J Biol Chem 1996;271:24313–24316.
[32] Liu ZG, Hsu H, Goeddel DV, Karin M. Dissection of TNF receptor 1 effector functions: JNK activation is not linked to apoptosis while NF-kappaB activation prevents cell death. Cell 1996;87:565–576.
[33] Lee HW, Choo MK, Bae EA, Kim DH. Beta-glucuronidase inhibitor tectorigenin isolated from the flower of *Pueraria thunbergiana* protects carbon tetrachloride-induced liver injury. Liver Int 2003;23:221–226.
[34] Rosenkranz AR, Schmaldienst S, Stuhlmeier KM, Chen W, Knapp W, Zlabinger GJ. A microplate assay for the detection of oxidative products using 2′,7′-dichlorofluorescein-diacetate. J Immunol Meth 1992;156:39–45.
[35] Lo SF, Nalawade SM, Mulabagal V, Matthew S, Chen CL, Kuo CL, Tsay HS. *In vitro* propagation by asymbiotic seed germination and 1,1-diphenyl-2-picrylhydrazyl (DPPH) radical scavenging activity studies of tissue culture raised plants of three medicinally important species of dendrobium. Biol Pharm Bull 2004;27:731–735.

[36] Ohkawa H, Ohishi N, Yagi K. Assay for lipid peroxides in animal tissues by thiobarbituric acid reaction. Anal Biochem 1979;95:351–358.
[37] Singh NP. Microgels for estimation of DNA strand breaks, DNA protein cross links and apoptosis. Mutat Res 2000;455:111–127.
[38] Rajagopalan R, Ranjan SK, Nair CK. Effect of vinblastine sulfate on gamma-radiation-induced DNA single-strand breaks in murine tissues. Mutat Res 2003;536:15–25.
[39] Carmichael J, DeGraff WG, Gazdar AF, Minna JD, Mitchell JB. Evaluation of a tetrazolium-based semiautomated colorimetric assay: Assessment of chemosensitivity testing. Cancer Res 1987;47:936–941.
[40] Nicoletti I, Migliorati G, Pagliacci MC, Grignani F, Riccardi C. A rapid and simple method for measuring thymocyte apoptosis by propidium iodide staining and flow cytometry. J Immunol Methods 1991;139:271–279.
[41] Rogakou EP, Pilch DR, Orr AH, Ivanova VS, Bonner WM. DNA double-stranded breaks induce histone H2AX phosphorylation on serine 139. J Biol Chem 1988;273:5858–5868.
[42] Karin M, Liu Z, Zandi E. AP-1 function and regulation. Curr Opin Cell Biol 1997;9:240–246.
[43] Kitamura M, Ishikawa Y, Moreno-Manzano V, Xu Q, Konta T, Lucio-Cazana J, Furusu A, Nakayama K. Intervention by retinoic acid in oxidative stress-induced apoptosis. Nephrol Dial Transplant 2002;17:84–87.
[44] Li L, Wang HK, Chang JJ, McPhail AT, McPhail DR, Terada H, Konoshima T, Kokumai M, Kozuka M, Estes JR. Rotenoids and isoflavones as cytotoxic constitutents from *Amorpha fruticosa*. J Nat Prod 1993;56:690–698.
[45] Bae EA, Han MJ, Lee KT, Choi JW, Park HJ, Kim DH. Metabolism of 6″-O-xylosyltectoridin and tectoridin by human intestinal bacteria and their hypoglycemic and *in vitro* cytotoxic activities. Biol Pharm Bull 1999;22:1314–1318.
[46] Valachovicova T, Slivova V, Bergman H, Shuherk J, Sliva D. Soy isoflavones suppress invasiveness of breast cancer cells by the inhibition of NF-kappaB/AP-1-dependent and -independent pathways. Int J Oncol 2004;25:1389–1395.
[47] Park EK, Shin YW, Lee HU, Lee CS, Kim DH. Passive cutaneous anaphylaxis-inhibitory action of tectorigenin, a metabolite of tectoridin by intestinal microflora. Biol Pharm Bull 2004;27:1099–1102.
[48] Kang KA, Lee KH, Chae S, Zhang R, Jung MS, Kim SY, Kim HS, Kim DH, Hyun JW. Cytoprotective effect of tectorigenin, a metabolite formed by transformation of tectoridin by intestinal microflora, on oxidative stress induced by hydrogen peroxide. Eur J Pharmacol 2005;519:16–23.
[49] Kitamura M, Ishikawa Y, Moreno-Manzano V, Xu Q, Konta T, Lucio-Cazana J, Furusu K, Nakayama. Intervention by retinoic acid in oxidative stress-induced apoptosis. Nephrol Dial Transplant 2002;17:84–87.